ANALYTICAL SCIENCES OCTOBER 2008, VOL. 24

2008 © The Japan Society for Analytical Chemistry

Use of Highly Hydrophobic Ionic Liquids for Ion-selective Electrodes of the Liquid Membrane Type

Naoya NISHI, Hiroshi MURAKAMI, Yukinori YASUI, and Takashi KAKIUCHI†

Department of Energy and Hydrocarbon Chemistry, Graduate School of Engineering, Kyoto University, Kyoto 615–8510, Japan

The phase-boundary potential at the interface between an aqueous KCl solution (W) and a hydrophobic room-temperature ionic liquid (RTIL), trioctylmethylammonium bis(nonafluorobutylsulfonyl)imide ([TOMA$^+$][$C_4C_4N^-$]), containing dicyclohexano-18-crown-6 (DCH18C6), shows the nernstian response to K^+ in W within a polarized potential window of 500 mV between [TOMA$^+$][$C_4C_4N^-$] and W, demonstrating that hydrophobic RTILs can be used as a nonvolatile ionic medium for liquid-membrane ion-selective electrodes. The complex formation constant of K^+ with DCH18C6 in [TOMA$^+$][$C_4C_4N^-$] is estimated to be on the order of 10^9 from the upper detection limit using a partition equilibrium model in the presence of a neutral ionophore. The response time of the phase-boundary potential is ~20 min. Gelled [TOMA$^+$][$C_4C_4N^-$] also shows the nernstian response to K^+, although the upper limit is lower probably due to a change in the solvent properties from the non-gelled [TOMA$^+$][$C_4C_4N^-$]. The response time of the gelled [TOMA$^+$][$C_4C_4N^-$] is ~5 min, shorter than that of the non-gelled [TOMA$^+$][$C_4C_4N^-$].

(Received June 4, 2008; Accepted July 16, 2008; Published October 10, 2008)

Introduction

Ion-selective electrodes (ISEs) of the liquid membrane type have been developed over four decades as sensitive, inexpensive and handy sensors to selectively determine the concentration (activity) of ions in aqueous samples.[1–3] The ISEs of this type sense any change in the phase-boundary potential determined by the partition equilibrium of ionic species in the vicinity of the interface between the liquid membrane and a sample solution.[4–7] The liquid membranes of the ISEs are usually composed of polymers, organic solvents, ion exchangers or salts of hydrophobic counter-ions, and ligands that specifically interact with the target ions.

Hydrophobic room-temperature ionic liquids (RTILs), which are composed of hydrophobic ions and immiscible with water, are attractive media for the liquid-membrane ion-selective electrodes because of their negligible volatility, ionic conductivity and hydrophobicity. However, the partition of the hydrophobic RTILs to an aqueous solution (W) may affect the phase-boundary potential for the RTIL–W two-phase systems.[8] The partition is useful when the phase-boundary potential formed by the partitioning of the RTIL is desirable as in the application of the RTILs to salt bridges.[9–11] However, the partition of RTIL-constituting ions should be minimized when the RTILs are used as so-called plasticizers or ion exchangers of the liquid-membrane ISEs. Several attempts have been made to use ILs as a component of the liquid-membrane ISEs.[12–14] In these studies the response of ISEs to the target ions was not nernstian; the slopes less than $(RT/z_iF)\ln 10$ were obtained for the plots of the potential against the common logarithm of the concentration of the target ions, where R is the gas constant, T is the absolute temperature, z_i is the charge on i in signed units of electronic charge, and F is the Faraday constant. One of the reasons for the non-ideal nernstian response is likely to be the insufficient hydrophobicity of the RTILs added to the membrane. The partition of the RTIL-constituent ions can make a non-negligible contribution to the phase-boundary potential between the liquid membrane and the aqueous solution.

The partition of RTIL-constituent ions can be minimized by using highly hydrophobic RTILs composed of highly hydrophobic ions. The interface between W and highly hydrophobic RTILs is electrochemically polarizable;[15–19] 1.1 V is the widest.[20] Within the wide polarized potential window, we found that alkali metal ions in W are able to be transferred into a highly hydrophobic ionic liquid, *N*-octadecylisoquinolinium tetrakis[3,5-bis(trifluoromethyl)phenyl]borate ([$C_{18}Iq^+$][$TFPB^-$]), containing a ligand, dibenzo-18-crown-6 (DB18C6), and be back-transferred from the [$C_{18}Iq^+$][$TFPB^-$], by controlling the phase-boundary potential across the [$C_{18}Iq^+$][$TFPB^-$]|W interface.[21]

These results suggest that ISEs based on highly hydrophobic RTILs as a plasticizer can be developed without the problem of a partition of the RTIL-constituent ions. During our voltammetric studies of the facilitated ion transfer (FIT) of metal ions with various ionophores, we found that a crown ether, dicyclohexano-18-crown-6 (DCH18C6), also facilitates the transfer of alkali metal ions into [$C_{18}Iq^+$][$TFPB^-$] within the polarized potential window at the [$C_{18}Iq^+$][$TFPB^-$]|W interface.[22] The FIT was observed for not only [$C_{18}Iq^+$][$TFPB^-$] but also many kinds of highly hydrophobic RTILs. In this paper, using a combination of a highly hydrophobic ionic liquid, trioctylmethylammonium bis(nonafluorobutylsulfonyl)imide ([TOMA$^+$][$C_4C_4N^-$]), DCH18C6 and K^+, we will show that the phase-boundary potential at the RTIL|W interface shows the nernstian response to K^+ in W.

† To whom correspondence should be addressed.
E-mail: kakiuchi@scl.kyoto-u.ac.jp

Experimental

Chemicals

Trioctylmethylammonium chloride ([TOMA$^+$]Cl$^-$, Tokyo Chemical Industry) and hydrogen bis(nonafluorobutylsulfonyl)-imide (H$^+$[$C_4C_4N^-$], Wako Pure Chemical Industries) were used for the preparation of [TOMA$^+$][$C_4C_4N^-$]. For voltammetry, lithium bis(nonafluorobutylsulfonyl)imide (Li$^+$[$C_4C_4N^-$], Central Glass) was used. For potentiometry, potassium bis(nonafluorobutylsulfonyl)imide (K$^+$[$C_4C_4N^-$], Tokyo Chemical Industry) and dicyclohexano-18-crown-6 (DCH18C6, Aldrich, a mixture of *cis-syn-cis* and *cis-anti-cis* isomers) were dissolved in [TOMA$^+$][$C_4C_4N^-$]. Poly(vinylidene fluoride-co-hexafluoropropylene) (P(VDF-HFP), with an average M_W of 400000, Aldrich) was used for the gellation of [TOMA$^+$][$C_4C_4N^-$]. All chemicals were used without further purification.

Preparation of [TOMA$^+$][$C_4C_4N^-$]

Equimolar amounts of [TOMA$^+$]Cl$^-$ and H$^+$[$C_4C_4N^-$] were dissolved in methanol. After evaporating methanol from the solution using an evaporator, the mixture ([TOMA$^+$][$C_4C_4N^-$] and HCl) was washed with water to remove HCl until Cl$^-$ ions were not detected when a $AgNO_3$ aqueous solution was added to the washing. Volatile impurities, such as methanol and water in [TOMA$^+$][$C_4C_4N^-$], were then evaporated using an oil pump.

Measurements of physicochemical properties

A differential scanning calorimeter (Pyris Diamond DSC, Perkin-Elmer) was used to determine the melting point and the glass transition point for [TOMA$^+$][$C_4C_4N^-$] at a heating rate of 10°C min^{-1} from –100°C. A pycnometer, a viscometer (TVE-22, Toki Sangyo), and an ionic conductometer (CM-117, Kyoto Electronics Manufacturing) was used for measurements of the density, the viscosity, and the ionic conductivity for [TOMA$^+$][$C_4C_4N^-$] at 25.0°C, respectively.

Cyclic voltammetry

Cyclic voltammograms at the [TOMA$^+$][$C_4C_4N^-$]|W interface were recorded using a previously described procedure.[18,23] The [TOMA$^+$][$C_4C_4N^-$]|W interface was formed at a micropipette tip with an inner diameter of between 20 and 30 μm. The two-electrode electrochemical cell employed was:

I	**II**	**III**	**IV**	**V**	
Ag/AgCl	100 mM LiCl 10 mM Li$^+$[$C_4C_4N^-$]	20 mmol kg^{-1} DCH18C6	10 mM KCl	Ag/AgCl	(A)
W_{ref}	(W_{ref})	([TOMA$^+$][$C_4C_4N^-$])	(W)		

where M denotes mol dm^{-3}. A micropipette filled with W (phase **IV**) was immersed in [TOMA$^+$][$C_4C_4N^-$] (phase **III**). A glass cylinder with an inner diameter of 0.5 mm and filled with W_{ref} (phase **II**), was also immersed in [TOMA$^+$][$C_4C_4N^-$] (phase **III**) as a counter electrode. Ag/AgCl wires were inserted into the micropipette and the glass cylinder. The voltage, E_v, was applied to the right-hand-side terminal (phase **V**) with respect to the left (phase **I**). The current, I, due to the transfer of cations from W to [TOMA$^+$][$C_4C_4N^-$] was taken to be positive.

Potentiometry

The response of the phase-boundary potential to K$^+$ in W for the [TOMA$^+$][$C_4C_4N^-$]–W two-phase system was studied using potentiometry. The potential was measured using an electrometer (R8140, Advantest) and a glass cell as described elsewhere.[8] The composition of the electrochemical cell employed was:

I	**II**	**III**	**IV**	**V**	
Ag/AgCl	2 mM KCl	180 mmol kg^{-1} DCH18C6 27 mmol kg^{-1} K$^+$[CC_4N^-]	x mM KCl	Ag/AgCl	(B)
	(W_{ref})	([TOMA$^+$][$C_4C_4N^-$])	(W)		

For the cell without the inner aqueous solution (W_{ref}), [TOMA$^+$][$C_4C_4N^-$] was gelled with P(VDF-HFP) and was coated to an Ag/AgCl wire.[11] The electrochemical cell was:

I	**II**	**III**	**IV**	
Ag/AgCl	4.2 wt% DCH18C6 3.5 wt% K$^+$[$C_4C_4N^-$] 31.5 wt% P(VDF-HFP) 60.8 wt% [TOMA$^+$][$C_4C_4N^-$]	x mM KCl (W)	Ag/AgCl	(C)

The molar ratio of DCH18C6 and K$^+$[$C_4C_4N^-$] to [TOMA$^+$][$C_4C_4N^-$] in phase **II** was 0.18 and 0.088, respectively. For cells (B) and (C) in potentiometry, the potential of the left-hand-side terminal with respect to the right is denoted as E_p. The x values for the concentration of KCl in W were 0.02, 0.05, 0.1, 0.2, 0.5, 1, 2, 5, 10, 20, 50, 100, 500, and 1000. A change in x gave rise to changes in the phase-boundary potential between W/AgCl/Ag as well as that between [TOMA$^+$][$C_4C_4N^-$] (or gelled [TOMA$^+$][$C_4C_4N^-$]) and W. To extract the change in the latter, E_p was corrected as follows:

$$E_{cor} = E_p - \frac{RT}{F} \ln a_{KCl}^{\pm}, \quad (1)$$

where E_{cor} is the corrected potential and $a_{KCl}^{\pm}$ is the mean ionic activity of KCl in W. For the values of the mean activity coefficient at concentrations higher than 0.1 M, literature values were used.[24] The values at concentrations lower than 0.1 M were estimated from the extended Debye–Hückel theory.[25]

All electrochemical measurements were performed at 25.0°C by circulating water in the outer jacket of the cells.

Results and Discussion

The physicochemical properties of water-saturated [TOMA$^+$][$C_4C_4N^-$] are shown in Table 1. RTILs based on $C_4C_4N^-$ and imidazolium-type cations have been reported,[26-28] but their physicochemical properties have not been available except those by thermal analysis.[26,28] The density for water-saturated [TOMA$^+$][$C_4C_4N^-$] at 25.0°C, 1.281 g cm^{-3}, is higher than those for RTILs composed of tetraalkylammonium ions and $C_1C_1N^-$ ions[29,30] and seems to be mainly due to the longer chain length of perfluoroalkyl moieties in $C_4C_4N^-$ compared with $C_1C_1N^-$. A similar and more systematic chain-length dependence of the density has been found for a series of RTILs based on perfluoroalkyltrifluoroborate ions.[31] The viscosity, 2.0 Pa s, is greater than that of tetraalkylammonium[$C_1C_1N^-$],[29,30] reflecting the larger size of $C_4C_4N^-$ than that of $C_1C_1N^-$. Similarly, the ionic conductivity, 12 μS cm^{-1}, is lower than that of tetraalkylammonium[$C_1C_1N^-$],[29,30] in harmony with the high viscosity.

Cyclic voltammograms (CVs) at the interface between [TOMA$^+$][$C_4C_4N^-$] and a 10 mM KCl aqueous solution recorded with cell (A) are shown in Fig. 1. In the absence of DCH18C6 (dotted curve), a charging current was observed within the polarized potential window. The width of the potential window was 500 mV. This is narrower than 800 mV at the [TOMA$^+$][TFPB$^-$]|W interface (at 56°C),[18] indicating that $C_4C_4N^-$ is less hydrophobic than TFPB$^-$.

Table 1 Physicochemical properties for water-saturated [TOMA$^+$][$C_4C_4N^-$] (melting point (T_m), glass transition point (T_g), density (d), viscosity (η), ionic conductivity (κ))

T_m/°C	T_g/°C	d/g cm^{-3} [a]	η/Pa s[a]	κ/μS cm^{-1} [a]
–1	75	1.281	2.0	12

a. At 25.0°C.

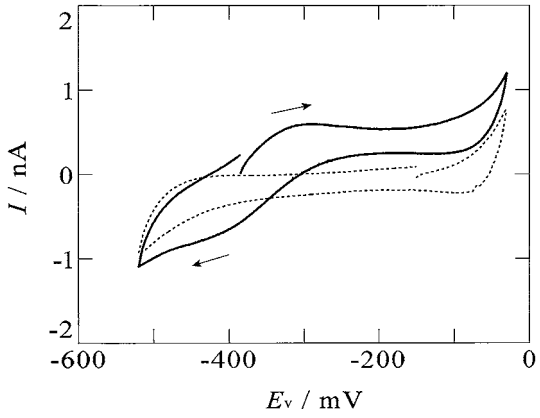

Fig. 1 Cyclic voltammograms for the ion transfer across the interface between a 10 mM KCl aqueous solution and [TOMA$^+$][$C_4C_4N^-$] in the presence (solid line) and the absence (dotted line) of 20 mmol kg^{-1} DCH18C6 in [TOMA$^+$][$C_4C_4N^-$]. Scan rate, 10 mV s^{-1}; inner diameter of the micropipette tip, 28 μm.

A CV in the presence of DCH18C6 (solid curve in Fig. 1) shows positive and negative currents superimposed on the charging current within the potential window. A positive and a negative current peak were seen at forward and backward scans, respectively. The feature is the same as that for the FIT of K^+ ions by DB18C6 across the [$C_{18}Iq^+$][TFPB$^-$]|W interface to form the 1:1 complex in [$C_{18}Iq^+$][TFPB$^-$] and is different from that for FIT of Cs^+ ions for the 1:2 (metal to ligand) complex where two peaks appear at forward and backward scans in the CV.[21] Therefore, we assumed that the positive and negative currents in CV correspond to those due to the FIT of K^+ ions by DCH18C6 to form the 1:1 complex in [TOMA$^+$][$C_4C_4N^-$] and the backward transfer, respectively. In several molecular solvents only the 1:1 complex was observed for K^+ and DCH18C6.[22,32-34] The FIT of K^+ from W to [TOMA$^+$][$C_4C_4N^-$] can be shown by the following equation:[35]

$$K^+(W) + L(R) \rightleftharpoons KL^+(R), \quad (2)$$

where L is a ligand, DCH18C6, KL^+ is the 1:1 complex of K^+ with DCH18C6, and R is RTIL. The Nernst equation of Eq. (1) may be written as[36,37]

$$\Delta_R^W\phi = \Delta_R^W\phi^0_{FIT} - \frac{RT}{F}\ln\frac{a_K^W a_L^R}{a_{KL}^R}, \quad (3)$$

where $\Delta_R^W\phi$ is the phase-boundary potential for the RTIL–W two-phase system, $\Delta_R^W\phi^0_{FIT}$ is the standard potential for Eq. (2), and a_i^α is the activity of i (i = K, L, KL) in the phase α (α = W, R). This equation means that $\Delta_R^W\phi$ shows the nernstian response to a_K^W as long as a_L^R and a_{KL}^R are unchanged. Such constancy of a_L^R and a_{KL}^R is established in potentiometry by dissolving a sufficient amount of DCH18C6 in [TOMA$^+$][$C_4C_4N^-$] and also a sufficient but less amount of K^+[$C_4C_4N^-$], as was suggested previously in a theoretical consideration of the potential of ISEs.[38]

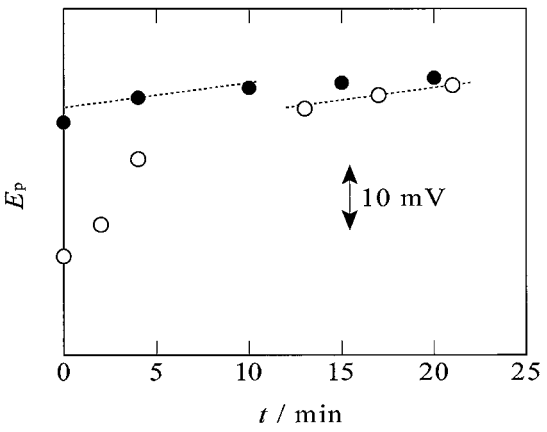

Fig. 2 Time dependence of the potential for cell (B) (open circle) and cell (C) (solid circle) at x = 1. The dotted lines represent lines with a slope of 0.5 mV min^{-1}.

In potentiometry we initially checked the response time of cells (B) and (C). Figure 2 shows a typical example of the time dependence of E_p for cell (B) using non-gelled [TOMA$^+$][$C_4C_4N^-$] (open circle). The time, t, in Fig. 2 was taken to be 0 when [TOMA$^+$][$C_4C_4N^-$] and W made contact with each other. E_p shifted to the positive direction in the first 20 min. The response time was approximately estimated from the time where $\Delta E_p/\Delta t$ becomes 0.5 mV min^{-1}, a criterion of the response time recommended by IUPAC.[39,40] The dotted lines in Fig. 2 are lines with a slope of 0.5 mV min^{-1}. The response time for cell (B) was ~20 min. A similar response time was obtained for other molar ratios of DCH18C6 to K^+[$C_4C_4N^-$]. The response time, ~20 min, is rather long compared with the order of minutes usually seen in ISEs of the liquid membrane type.[40] The time dependence of E_p for cell (C) with the gelled [TOMA$^+$][$C_4C_4N^-$] and without the W_{ref} phase is also shown in Fig. 2 (solid circle). The response time for cell (C) was ~5 min, shorter than that for cell (B). One reason of the longer response time of cell (B) may be the transfer of K^+ and Cl^- ions from W (W_{ref}) to W_{ref} (W) to reach a three-phase equilibration for W/[TOMA$^+$][$C_4C_4N^-$]/W_{ref} phases. However, the effect of the possible ion transfer on E_p after a long time seems to be negligible, judging from the nernstian response found for cell (B) (*vide infra*). Another possible reason for the response times common to cells (B) and (C) is a slow structural change of the electrical double layer (EDL) at the RTIL side of the RTIL|W interface to a phase-boundary potential change, which we recently found by electrocapillarity measurements at the [TOMA$^+$][$C_4C_4N^-$]|W interface and other RTIL|W interfaces.[41] Hereafter, for the plot of the potentials against the mean ionic activity of K^+ in W, we used the potentials at $t \geq 30$ min.

The variation of the potential against the common logarithm of the activity of K^+ in W for cell (B) is shown in Fig. 3. The plot of E_{cor} *vs.* log $a^{\pm}_{KCl}$ is linear in the concentration range from 50 μM to 100 mM. The linear relationship agrees with a slope of 59.2 mV/decade at 25°C shown in Fig. 3 as a solid line. At lower and higher concentrations beyond this concentration range, the experimental points deviated from the nernstian slope. One possible reason for the deviation at low concentrations is the shift of the potential of the Ag/AgCl/W interface from the expected one due to low Cl^- concentrations.[10] Another reason for the deviation is the dissolution of AgCl in W from the Ag/AgCl

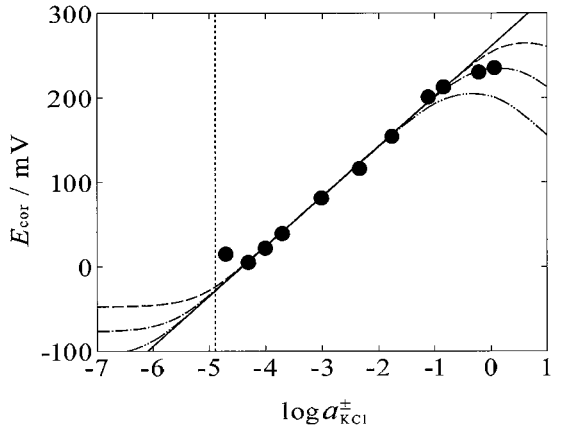

Fig. 3 Plots of E_{cor} against log $a^{\pm}_{KCl}$ for the KCl aqueous solution–[TOMA$^+$][$C_4C_4N^-$] (containing DCH18C6 and K$^+$[$C_4C_4N^-$]) two-phase system represented as cell (B) at various concentrations of KCl in an aqueous solution. The solid line represents a line with the nernstian slope at 25°C (59.2 mV/decade). Three curves are from a calculation of the phase-boundary potential with $K_{ML} = 1 \times 10^8$ (dashed line) 1×10^9 (dashed dotted line), and 1×10^{10} (dashed double-dotted line) and other fixed parameters (see Table 2). The vertical dotted line shows the solubility of AgCl in water (13 μmol dm^{-3}).

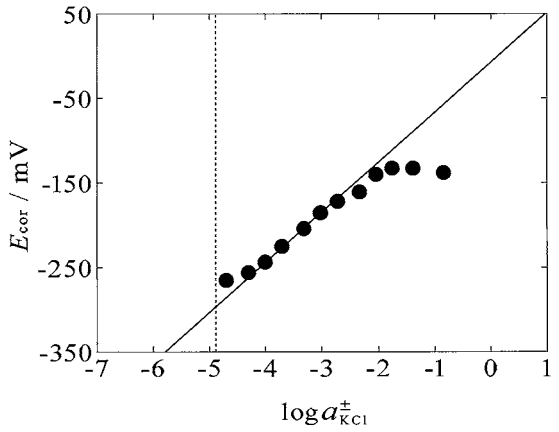

Fig. 4 Plots of E_{cor} against log $a^{\pm}_{KCl}$ for the KCl aqueous solution–gelled [TOMA$^+$][$C_4C_4N^-$] (containing DCH18C6 and K$^+$[$C_4C_4N^-$]) two-phase system represented as cell (C) at various concentrations of KCl in the aqueous solution. The solid line represents a line with the nernstian slope at 25°C (59.2 mV/decade). The vertical dotted line shows the solubility of AgCl in water (13 μmol dm^{-3}).

Table 2 Values of parameters used in calculating phase-boundary potential

Parameter	Value
$\Delta^W_R\phi^{0'}_K$	+0.24 V[a]
$\Delta^W_R\phi^{0'}_{Cl}$	–0.39 V[a]
$\Delta^W_R\phi^{0'}_{TOMA}$	–0.51 V[b]
$\Delta^W_R\phi^{0'}_{C4C4N}$	+0.35 V[c]
$c^{R,0}_{KC4C4N}$	0.027 mol dm^{-3} [d]
$c^{R,0}_{L}$	0.18 mol dm^{-3} [d]
$c^{R,0}_{TOMAC4C4N}$	1.35 mol dm^{-3} [e]
r	1
K_{ML}	1×10^9 [f]

a. From literature values of $\Delta^W_{NB}\phi^{0'}_i$.[47,48]
b. Extrapolated from the dependence of $\Delta^W_{NB}\phi^{0'}_i$ for symmetrical tetraalkylammonium ions (from methyl to hexyl)[49] on the alkyl chain length of the cations.
c. Extrapolated from the dependence of $\Delta^W_{NB}\phi^{0'}_i$ for $C_nC_mN^-$[50] on the perfluoroalkyl chain length of the anions.
d. Approximated to be equal to the molality in the conditions shown in cell (B).
e. Calculated from the density and formula weight of [TOMA$^+$][$C_4C_4N^-$].
f. The cases with $K_{ML} = 1 \times 10^8$ or 1×10^{10} are also shown in Fig. 3.

electrode to produce Ag$^+$ ions in W behaving as interfering ions to K$^+$. The AgCl dissolution occurs when the Cl$^-$ concentration is lower than or compatible with 13 μM, the solubility of AgCl in water.[42] The complex formation constant with DCH18C6 of Ag$^+$ is known to be comparable to that of K$^+$ in molecular solvents,[32] suggesting that the lower limit in the present study is located at concentrations around the solubility of AgCl.

The deviation at high concentrations in Fig. 3 can be interpreted by assuming that the partition of KCl in W into [TOMA$^+$][$C_4C_4N^-$] occurs at high concentrations.[38] Such an upper limit is determined by several factors such as the hydrophobicity of the metal ion and the counter-ion in W, and the complex formation constant of the metal ion with the ligand in liquid membranes of ISEs.[38] We employed a model to explain the upper limit and to evaluate the complex formation constant of K$^+$ with DCH18C6 in [TOMA$^+$][$C_4C_4N^-$]. In the present study, the complex formation constant of K$^+$ with DCH18C6 was a weighted average of that of the *cis-syn-cis* and *cis-anti-cis* isomers. It is known that these *cis* isomers show almost the same extractability of metal ions,[43] while the difference in *cis* and *trans* isomers is much larger.[32,43] In the model adopted,[44,45] the phase-boundary potential at equilibrium is calculated using several parameters including the formal potential for the ion transfer across the RTIL|W interface, $\Delta^W_R\phi^{0'}_i$, for all ions in the two-phase system and the complex formation constant (see Appendix for details).

In the following we used the formal potential of the ion transfer across the nitrobenzene (NB)|W interface, $\Delta^W_{NB}\phi^{0'}_i$, for approximate values of $\Delta^W_R\phi^{0'}_i$, because $\Delta^W_{NB}\phi^{0'}_i$ has been shown to be a good measure of $\Delta^W_R\phi^{0'}_i$ for imide-based RTILs[15] and RTILs based on other anions.[30] The parameters used to calculate the phase-boundary-potential for the RTIL-W two-phase system, $\Delta^W_R\phi$, are listed in Table 2. The volume ratio of RTIL to W, r, can significantly affect the partition characteristics, especially when r is extremely large or small, for example, in the cases of emulsions or vesicles.[46] In the present study r was assumed to be unity.

E_{cor}–log $a^{\pm}_{KCl}$ curves from the calculation with the complex formation constants of 1×10^8 (dashed line), 1×10^9 (dashed dotted line) and 1×10^{10} (dashed double-dotted line) are shown in Fig. 3. One can see that the curve with 1×10^9 is well fitted to experimental plots at high concentrations of K$^+$. At the lower limit the calculation curves did not fit to the experimental plots because neither the unexpected shift of the Ag/AgCl electrode nor the interference by Ag$^+$ was taken into account in the calculation. From Fig. 3, one can see that the value of the complex formation constant is on the order of 10^9, which agrees with 1×10^9, for the same complexation in nitrobenzene evaluated using cyclic voltammetry for the ion transfer across the NB|W interface.[22]

The response of cell (C) using the gelled [TOMA$^+$][$C_4C_4N^-$] is shown in Fig. 4. The linear relationship between E_{cor} and log $a^{\pm}_{KCl}$ was from 50 μM to 10 mM. The lower limit of the nernstian response is similar to that in the non-gelled [TOMA$^+$][$C_4C_4N^-$] in Fig. 3. The upper limit decreased from 100 to 10 mM. This is likely to be caused by a change in the

properties of [TOMA$^+$][$C_4C_4N^-$] as a solvent by gellation; $\Delta^W_R\phi^{0'}_i$ and the complex formation constant in gelled RTILs can vary from those in the non-gelled RTILs.

Conclusions

It has been demonstrated that the phase-boundary potential for the [TOMA$^+$][$C_4C_4N^-$]-water two-phase system in the presence of DCH18C6 shows the nernstian response to K^+ in water. This response is achieved by the high hydrophobicity of TOMA$^+$ and $C_4C_4N^-$. Within the potential window shown in the CVs, the solubility of [TOMA$^+$][$C_4C_4N^-$] is negligible, so that the phase-boundary potential remains unaffected. The nernstian concentration range, from 10^{-5} to 10^{-1} M for the non-gelled [TOMA$^+$][$C_4C_4N^-$] and from 10^{-5} to 10^{-2} M for the gelled [TOMA$^+$][$C_4C_4N^-$], is promising in practical applications of this type of ISEs. ISEs based on gelled RTILs allow us to miniaturize the ISE by combining RTIL-based reference electrodes recently proposed.[11]

Appendix

The phase-boundary potential for an oil(O)–water(W) two-phase system, $\Delta^W_O\phi$, determined by the ion partitioning can be calculated by knowing the initial concentrations of all chemical species, the formal potential of the ion transfer across the O|W interface, $\Delta^W_O\phi^{0'}_i$, the volume ratio of O to W, r, and the formation constants for ion pairs or complexes.[44-46] This Appendix describes the method for calculating $\Delta^W_O\phi$ in the case when the W phase contains metal ions and the O phase contains neutral ligands and complexes of the ions with the ligands at the initial state, as are in the usual cases of ISEs.

When the ion-partition equilibrium of n kinds of ionic species (i) is established between the W and O phases, the Nernst equations for each ion hold:

$$\frac{c^O_i}{c^W_i} = \exp\frac{z_iF}{RT}(\Delta^W_O\phi - \Delta^W_O\phi^{0'}_i) \equiv e'_i \quad (i = 1, \cdots, n), \tag{4}$$

where c^α_i is the concentration of i in the α phase (α = W or O) at equilibrium. The equations for the mass conservation of n kinds of ionic species are

$$c^W_i + rc^O_i = c^{W,0}_i + rc^{O,0}_i \quad (i = 1, \cdots, n), \tag{5}$$

where $c^{\alpha,0}_i$ is the concentration of i in the α phase in the initial state. By neglecting the charge imbalance in the narrow electric double layer region, the electroneutrality for each phase is represented as

$$\sum_i z_ic^\alpha_i = 0 \quad (\alpha = \text{W or O}). \tag{6}$$

By eliminating c^α_i from Eqs. (4) - (6), one obtains a polynomial equation of $\Delta^W_O\phi$ for the case without complexation:[44-46]

$$\sum_i \frac{z_i(c^{W,0}_i + rc^{O,0}_i)}{1 + re'_i} = 0. \tag{7}$$

The value of the phase-boundary potential at equilibrium $\Delta^W_O\phi$ is obtained by solving Eq. (7).

For the case in the presence of the complexation between a ligand and metal ions, we need to modify Eq. (7) for the metal ion, M, involved in the complexation. We assume that M makes only a 1:1 complex, ML, with a neutral ligand, L, only in the O phase and that ML and L initially dissolved in the O phase are not partitioned to the W phase. The equation of the mass conservation for M is modified to that for M-related species (M and ML) shown as

$$c^W_M + rc^O_M + rc^O_{ML} = c^{W,0}_M + rc^{O,0}_{M,t}, \tag{8}$$

where $c^{\alpha,0}_{i,t}$ is the total concentration of i in α in the initial state. Similarly, mass conservation for L-related species (ML and L) leads to

$$c^O_{ML} + c^O_L = c^{O,0}_{L,t}. \tag{9}$$

The complex formation constant, K_{ML}, is represented as

$$K_{ML} = \frac{c^O_{ML}}{c^O_Mc^O_L}. \tag{10}$$

From Eqs. (8) - (10), one obtains c^W_M as a function of $\Delta^W_O\phi$ (*via* e'_M),

$$c^W_M = \frac{-p + \sqrt{p^2 + 4q}}{2}, \tag{11}$$

where

$$p = \frac{1}{K_{ML}e'_M} - \frac{c^{W,0}_M + rc^{O,0}_{M,t} - rc^{O,0}_{L,t}}{1 + re'_M} \tag{12}$$

$$q = \frac{c^{W,0}_M + rc^{O,0}_{M,t}}{K_{ML}e'_M(1 + re'_M)}. \tag{13}$$

Thus, Eq. (7) can be modified for this complexation system, as

$$\sum_{i\neq M} \frac{z_i(c^{W,0}_i + rc^{O,0}_i)}{1 + re'_i} + z_M\frac{-p + \sqrt{p^2 + 4q}}{2} = 0. \tag{14}$$

With known values of $c^{\alpha,0}_i$ and $\Delta^W_O\phi^{0'}_i$ for all ions and other parameters related to complexation ($c^{O,0}_{M,t}$, $c^{O,0}_{L,t}$ and K_{ML}), this polynomial equation for $\Delta^W_O\phi$ can be numerically solved. The curves shown in Fig. 3 were calculated using Eq. (14) and the values are given in Table 2.

Acknowledgements

This work was partially supported by a Grant-in-Aid for Scientific Research (No. 14205120), a Grant-in-Aid for Exploratory Research (No. 15655008) and a Grant-in-Aid for Young Scientists (No. 16750060) from the Ministry of Education, Culture, Sports, Science and Technology (MEXT), Japan, and by the Global COE Program "International Center for Integrated Research and Advanced Education in Materials Science" (No. B-09) of MEXT.

References

1. J. Koryta, *Anal. Chim. Acta*, **1972**, *61*, 329.
2. E. Bakker, P. Bühlmann, and E. Pretsch, *Chem. Rev.*, **1997**, *97*, 3083.
3. E. Lindner and Y. Umezawa, *Pure Appl. Chem.*, **2008**, *80*, 85.
4. K. Cammann in "*Ion-selective Electrodes*", ed. E. Pungor and I. Buzás, **1978**, Elsevier.

5. T. Kakiuchi and M. Senda, *Bull. Chem. Soc. Jpn.*, **1984**, *57*, 1801.
6. S. Kihara and Z. Yoshida, *Talanta*, **1984**, *31*, 789.
7. T. Kakiuchi, I. Obi, and M. Senda, *Bull. Chem. Soc. Jpn.*, **1985**, *57*, 1636.
8. T. Kakiuchi, N. Tsujioka, S. Kurita, and Y. Iwami, *Electrochem. Commun.*, **2003**, *5*, 159.
9. T. Kakiuchi and T. Yoshimatsu, *Bull. Chem. Soc. Jpn.*, **2006**, *79*, 1017.
10. T. Yoshimatsu and T. Kakiuchi, *Anal. Sci.*, **2007**, *23*, 1049.
11. T. Kakiuchi, T. Yoshimatsu, and N. Nishi, *Anal. Chem.*, **2007**, *79*, 7187.
12. C. Coll, R. H. Labrador, R. M. Mañez, J. Soto, F. Sancenón, M.-J. Seguí, and E. Sanchez, *Chem. Commun.*, **2005**, 3033.
13. N. V. Shvedene, D. V. Chernyshov, M. G. Khrenova, A. A. Formanovsky, V. E. Baulin, and I. V. Pletnev, *Electroanalysis*, **2006**, *18*, 1416.
14. C. Wardak, J. Lenik, and B. Marczewska, *Pol. J. Chem.*, **2008**, *82*, 223.
15. T. Kakiuchi and N. Tsujioka, *Electrochem. Commun.*, **2003**, *5*, 253.
16. H. Katano and H. Tatsumi, *Anal. Sci.*, **2003**, *19*, 651.
17. T. Kakiuchi, N. Tsujioka, K. Sueishi, N. Nishi, and M. Yamamoto, *Electrochemistry*, **2004**, *72*, 833.
18. N. Nishi, S. Imakura, and T. Kakiuchi, *Anal. Chem.*, **2006**, *78*, 2726.
19. J. Langmaier and Z. Samec, *Electrochem. Commun.*, **2007**, *9*, 2633.
20. R. Ishimatsu, N. Nishi, and T. Kakiuchi, *Chem. Lett.*, **2007**, *36*, 1166.
21. N. Nishi, H. Murakami, S. Imakura, and T. Kakiuchi, *Anal. Chem.*, **2006**, *78*, 5805.
22. H. Murakami, Master Thesis, Department of Energy and Hydrocarbon Chemistry, Graduate School of Engineering, Kyoto University, **2007**.
23. N. Tsujioka, S. Imakura, N. Nishi, and T. Kakiuchi, *Anal. Sci.*, **2006**, *22*, 667.
24. R. Robinson and R. Stokes, "*Electrolyte Solutions*", 1st ed., **1955**, Butterworths, London.
25. H. S. Harned and B. B. Owen, "*The Physical Chemistry of Electrolyte Solutions*", 3rd ed., **1958**, Reinhold, New York.
26. J. Zhang, G. R. Martin, and D. D. DesMarteau, *Chem. Commun.*, **2003**, *395*, 2334.
27. K. Driesen, P. Nockemann, and K. Binnemans, *Chem. Phys. Lett.*, **2004**, *395*, 306.
28. S. K. Quek, I. M. Lyapkalo, and H. V. Huynh, *Tetrahedron*, **2006**, *62*, 3137.
29. H. Matsumoto, H. Kageyama, and Y. Miyazaki, *Chem. Lett.*, **2001**, 182.
30. N. Nishi, T. Kawakami, F. Shigematsu, M. Yamamoto, and T. Kakiuchi, *Green Chem.*, **2006**, *8*, 349.
31. Z.-B. Zhou, H. Matsumoto, and K. Tatsumi, *Chem.—Eur. J.*, **2004**, *10*, 6581.
32. H. K. Frensdorff, *J. Am. Chem. Soc.*, **1971**, *93*, 600.
33. H.-J. Buschmann, *Chem. Ber.*, **1985**, *118*, 2746.
34. Y. Kikuchi and Y. Sakamoto, *Anal. Chim. Acta*, **2000**, *403*, 325.
35. J. Koryta, *Electrochim. Acta*, **1979**, *24*, 293.
36. E. A. Guggenheim, *J. Phys. Chem.*, **1929**, *33*, 842.
37. D. Homolka, K. Holub, and V. Mareček, *J. Electroanal. Chem.*, **1982**, *138*, 29.
38. E. Bakker, A. Xu, and E. Pretsch, *Anal. Chim. Acta*, **1994**, *295*, 253.
39. R. P. Buck and E. Lindner, *Pure Appl. Chem.*, **1994**, *66*, 2527.
40. C. Maccà, *Anal. Chim. Acta*, **2004**, *512*, 183.
41. Y. Yasui, Y. Kitazumi, R. Ishimatsu, N. Nishi, M. Yamamoto, and T. Kakiuchi, in Proceedings of the 69th Spring Meeting of the Japan Society for Analytical Chemistry, **2008**, Nagoya, Japan, 103.
42. W. E. Waghorne, *Monatsh. Chem.*, **2003**, *134*, 655.
43. M. L. Dietz, S. Jakab, K. Yamato, and R. A. Bartsch, *Green Chem.*, **2008**, *10*, 174.
44. L. Q. Hung, *J. Electroanal. Chem.*, **1980**, *115*, 159.
45. L. Q. Hung, *J. Electroanal. Chem.*, **1983**, *149*, 1.
46. T. Kakiuchi, *Anal. Chem.*, **1996**, *68*, 3658.
47. J. Rais, *Collect. Czech. Chem. Commun.*, **1971**, *36*, 3253.
48. B. Hundhammer and S. Wilke, *J. Electroanal. Chem.*, **1989**, *266*, 133.
49. Z. Samec, D. Homolka, V. Mareček, and L. Kavan, *J. Electroanal. Chem.*, **1983**, *145*, 213.
50. S. Tanaka, Y. Kitazumi, Y. Matsuoka, N. Nishi, and T. Kakiuchi, in preparation.